Results (Clean Projections)

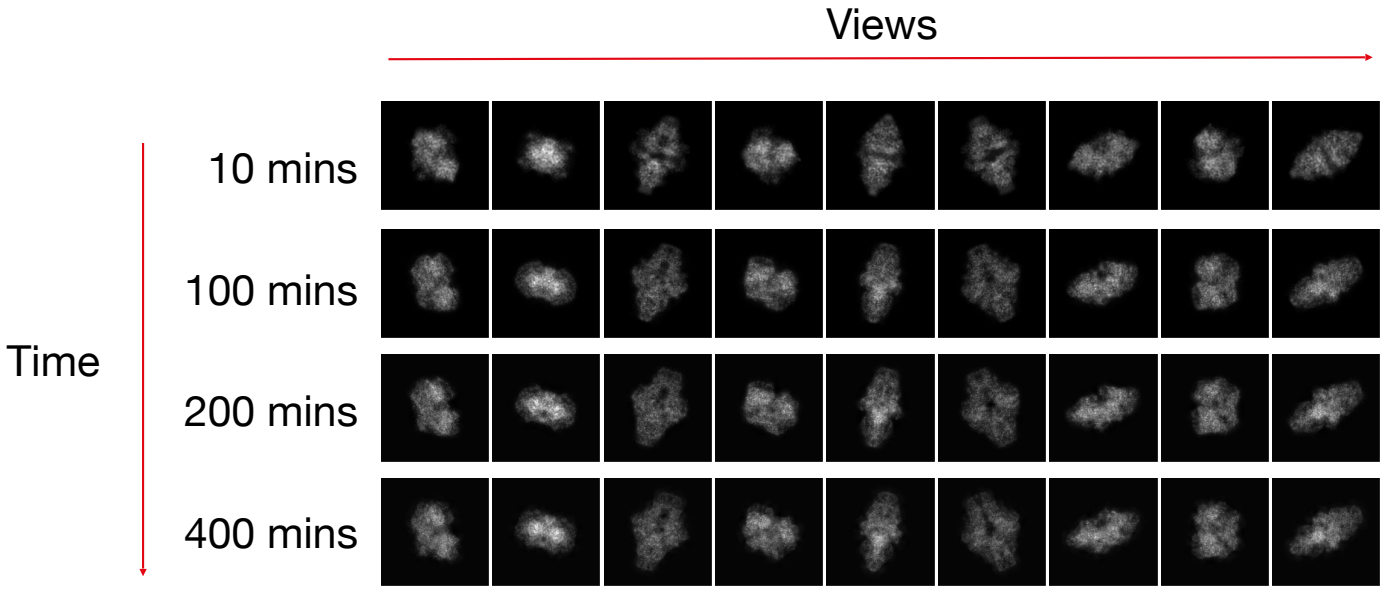

Results (Final projections)

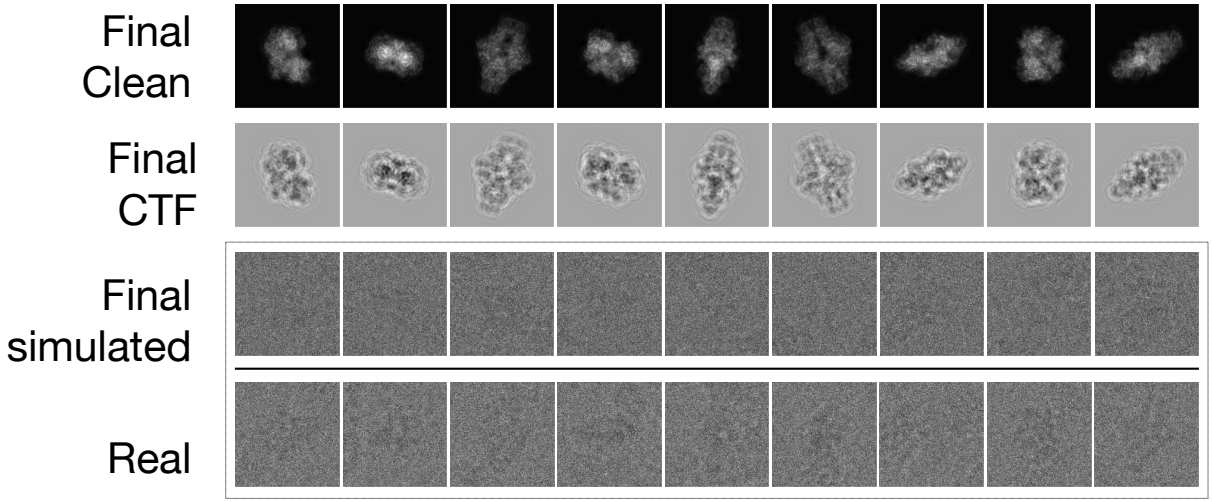

Experimental data (EMPIAR-10061)

- CTF estimated
- Uniform distribution assumed
- Noise extracted from micrograph background

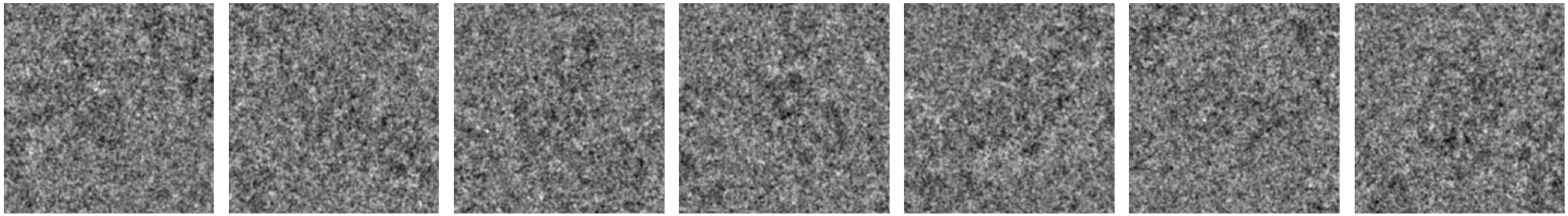

Reconstruction (Structure)

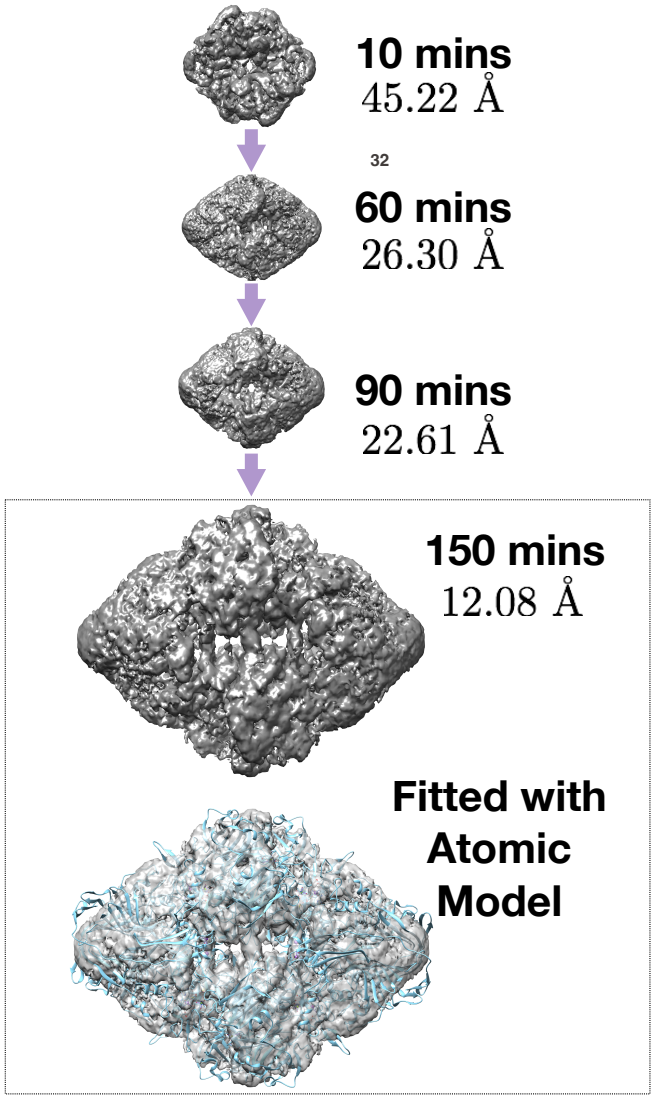

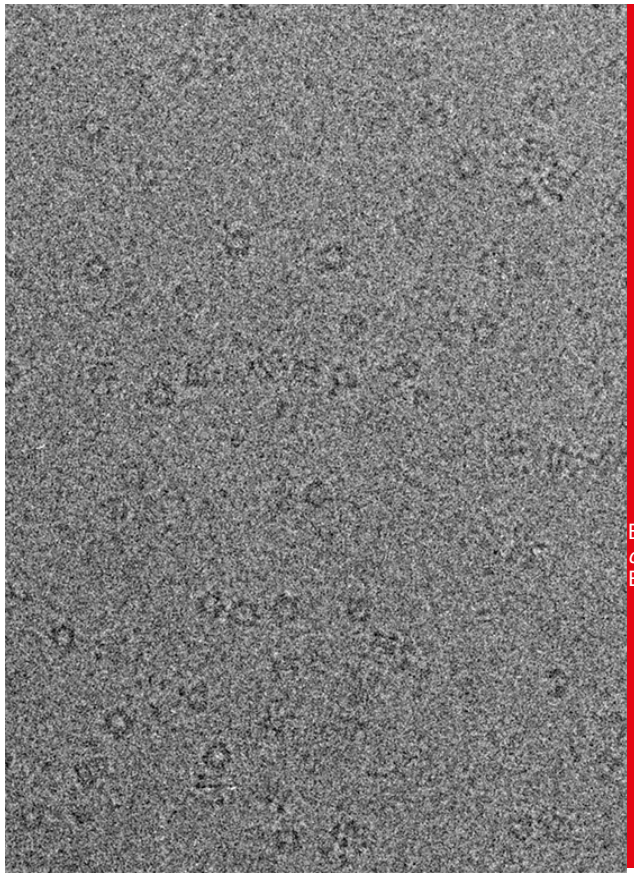

Multi CryoGAN for continuous conformations

Based on: **Gupta**, Phan, Yoo, Unser, ``*Multi-CryoGAN: Reconstruction of continuous conformations in Cryo-EM using Generative Adversarial Networks*,'' ECCV Workshop on BioImage Computing (BIC), August 2020.

Multi-CryoGAN: General idea

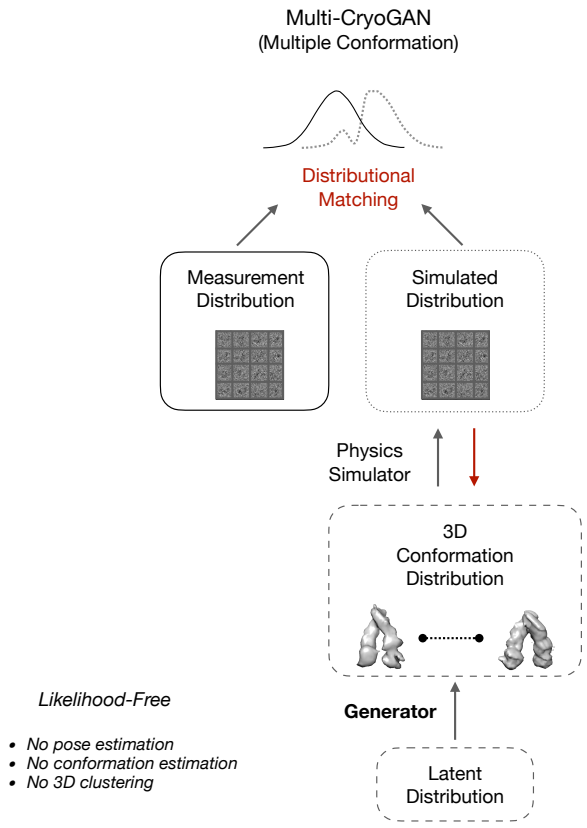

- No pose/conformation estimation
- Continuous/discrete conformation manifold reconstruction
- Guarantee of recovery of true conformations

[Theorem 1, Gupta et al. 2020]

Multi-CryoGAN: details

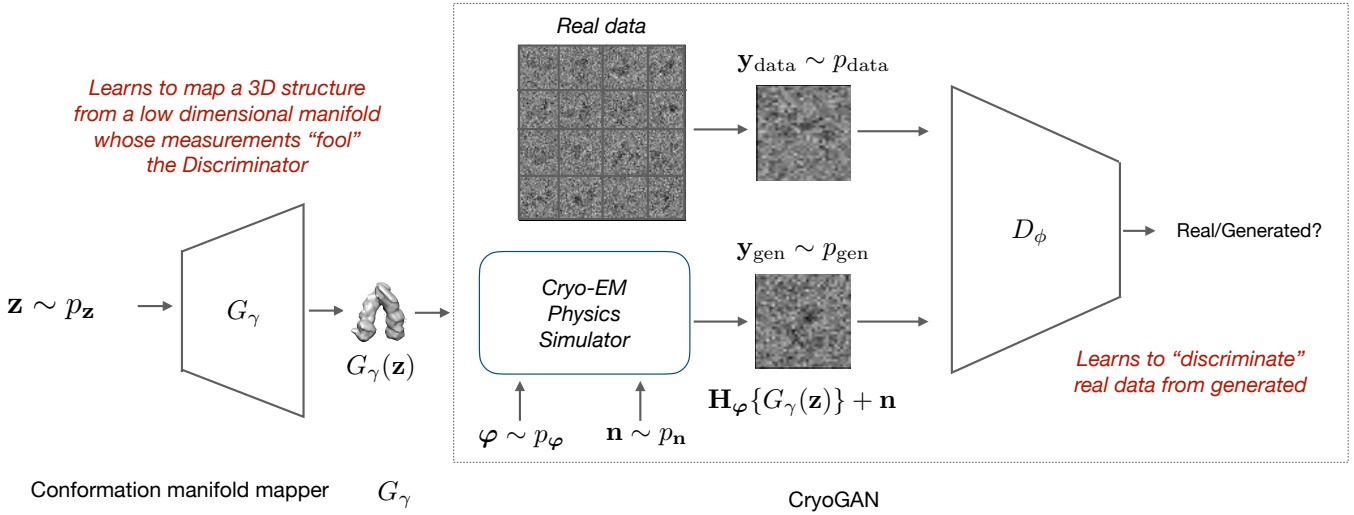

- Could be viewed as standard WGAN structure with a physics simulator in the generator
- Generator transforms latent distribution into conformation distribution

Datasets

Use part of the framework from (Seitz, Acosta-Reyes, Schwander, Frank, 2019):

- Heat shock protein Hsp90

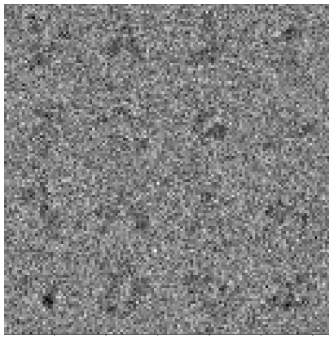

2 datasets:

- Continuous conformation
- Discrete conformation:

- 1e5 projections (32 x 32) in each dataset
- CTF modulated
- Gaussian noise -10 dB

- Latent distribution is uniform on a 1D line

Reconstruction

Ground truth

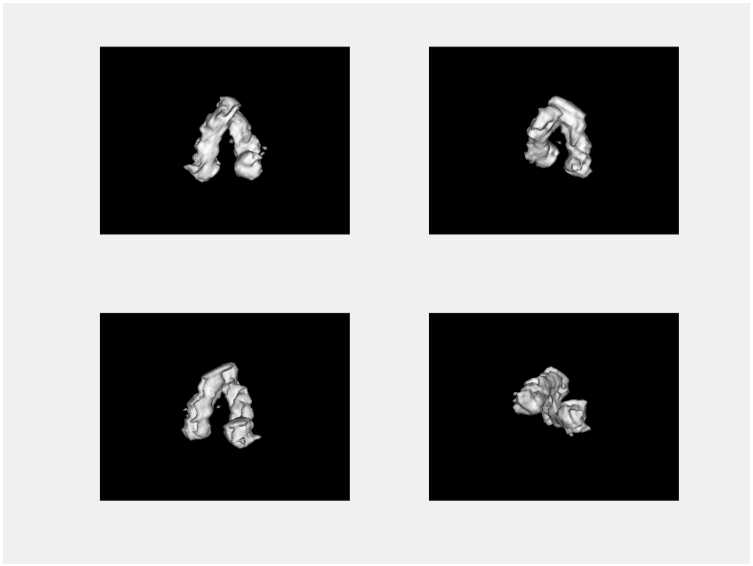

Reconstruction (at different views)

Reconstruction

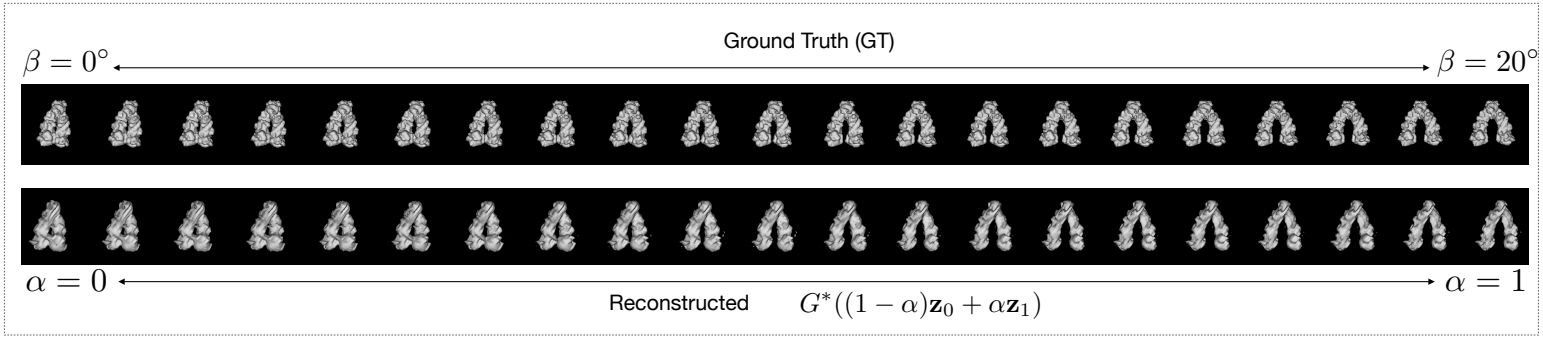

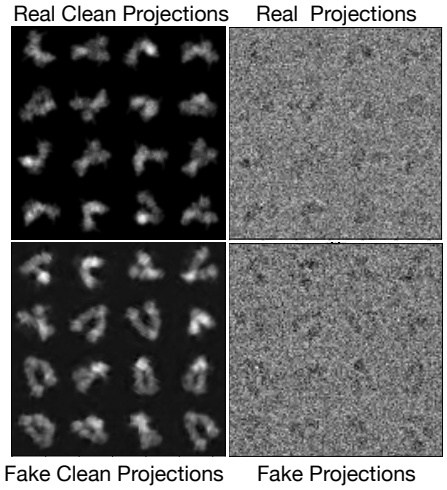

Reconstruction

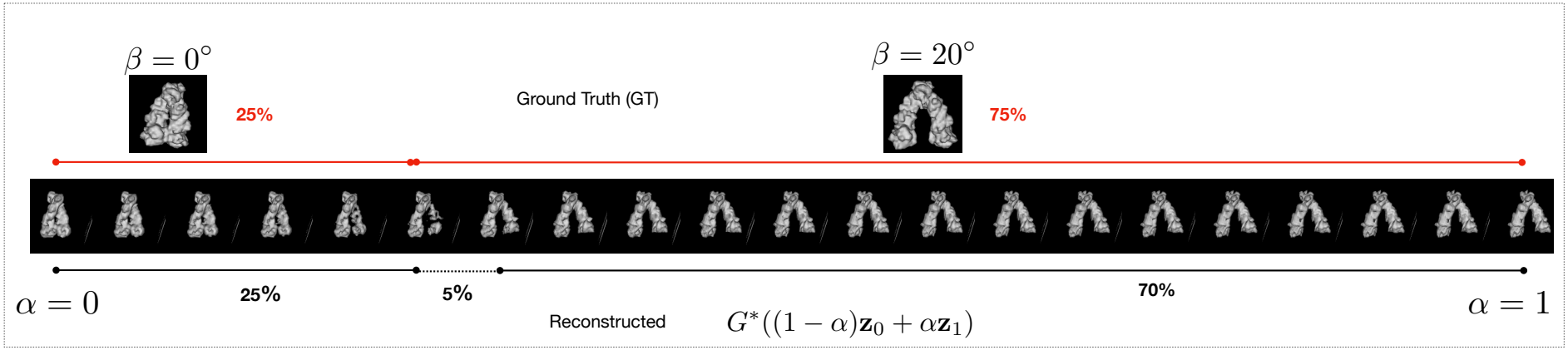

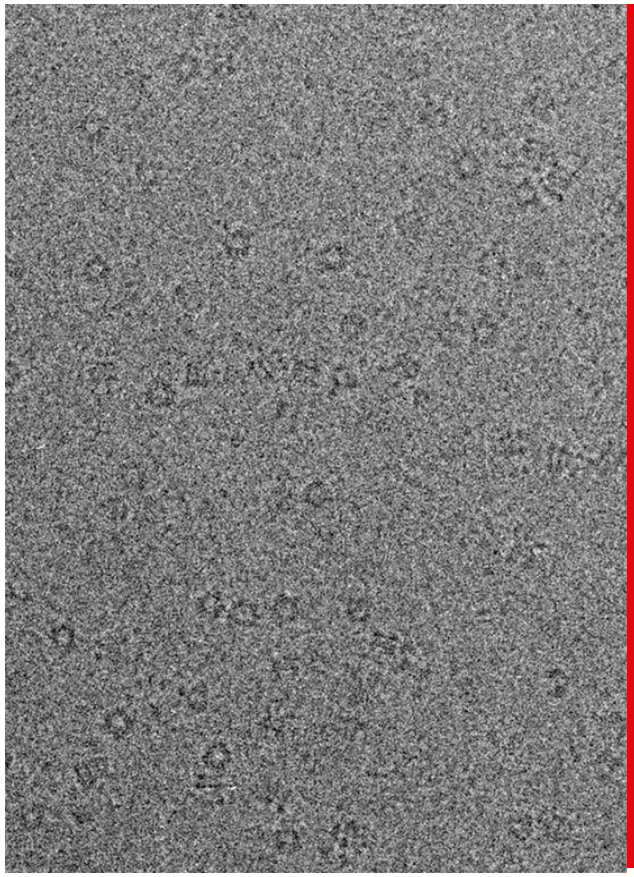

CryoGAN vs Likelihood

CryoGAN vs Likelihood methods

- Max-likelihood

$$\mathbf{x}_{\text{rec}} = \arg\max_{\mathbf{x}} \sum_{n=1}^{N} \log p(\mathbf{y}^n_{\text{data}}|\mathbf{x})$$

- KL-Divergence

$$\mathbf{x}_{\text{rec}} = \arg\min_{\mathbf{x}} KL(p_{\text{data}}(\mathbf{y})||p(\mathbf{y}|\mathbf{x}))$$

$$\mathbf{x}_{\text{rec}} = \arg\min_{\mathbf{x}} \mathbb{E}_{\mathbf{y}\sim p_{\text{data}}}\left[\log \frac{p_{\text{data}}(\mathbf{y})}{p(\mathbf{y}|\mathbf{x})}\right]$$

Need to calculate $p(\mathbf{y}|\mathbf{x})$.

Wasserstein Distance

$$\mathbf{x}_{\text{rec}} = \operatorname{argmin}_{\mathbf{x}} \inf_{\gamma\in\Pi(p_{\mathbf{x}},p_{\text{data}})} \mathbb{E}_{(\mathbf{y}_1,\mathbf{y}_2)\sim\gamma}[\|\mathbf{y}_1 - \mathbf{y}_2\|]$$

$$\mathbf{x}_{\text{rec}} = \operatorname{argmin}_{\mathbf{x}} \max_{\mathbf{D}_\phi:\|\mathbf{D}_\phi\|_L<1} \left(\mathbb{E}_{\mathbf{y}\sim p_{\text{data}}}[\mathbf{D}_\phi(\mathbf{y})] - \mathbb{E}_{\mathbf{y}\sim p_{\mathbf{x}}}[\mathbf{D}_\phi(\mathbf{y})]\right)$$

Just require a sampler from the distributions

Theoretically both are the same (distributional matching) but one is explicit and one is implicit!!

Conclusion

- CryoGAN/MultiCryoGAN is a deep adversarial learning scheme.
- Does not need likelihood computation or pose and conformation estimation/marginalization.
- Theoretically can recover the ground truth.
- Similar to GANs but with a physics-based generator instead of neural-network-based generator.
- Best of both learning-based and model-based approaches.
- For single conformations works reasonable on synthetic experiments (7-8 A).
- For multiple conformation needs to be deployed on real data
- Multi-resolution approach would improve results

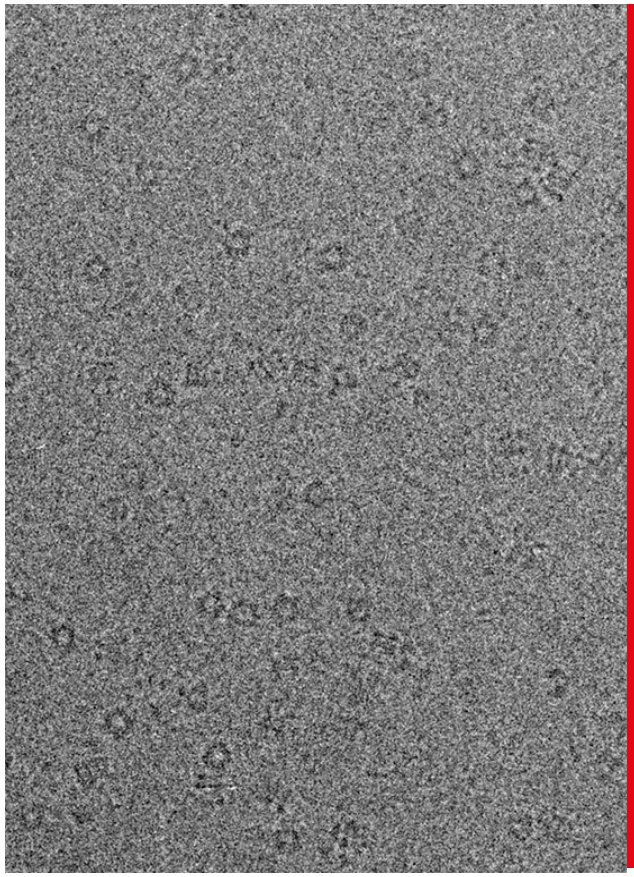

References

References

- J Adler, O Oktem. "*Solving ill-posed inverse problems using iterative deep neural networks*". Inverse Problems, 2018.
- K. C. Tezcan, C. F. Baumgartner, R. Luechinger, K. P. Pruessmann, and E. Konukoglu, "*MR image reconstruction using deep density priors*," IEEE TMI, 2019.
- Y.Chun and J.A. Fessler,"*Deep bcd-net using identical encoding-decoding cnn structures for iterative image recovery*," IVMSP, 2018.
- K.Hammernik, T.Klatzer,E.Kobler, M.Recht, D.Sodickson, T.Pock *etal*.,"*Learning a variational network for reconstruction of accelerated MRI data*," *MRM,* 2018.
- J.Rick Chang, C.-L.Li, B.Poczos, B.VijayaKumar, and A.C. Sankaranarayanan,"*One network to solve them all–solving linear inverse problems using deep projection models*," ICCV 2018.
- V. Lempitsky, A.Vedaldi, and D.Ulyanov, "*Deep image prior*," CVPR, 2018.
- I.Goodfellow, J.Pouget-Abadie, M.Mirza, B.Xu, D.Warde-Farley, S.Ozair, A.Courville, and Y. Bengio, "*Generative adversarial nets*," NeurIPS, 2014.
- M. Vulovic´, R. B. Ravelli, L. J. van Vliet, A. J. Koster, I. Lazic´, U. Lücken, H. Rullgård, O. Öktem, and B. Rieger, "*Image formation modeling in cryo-electron microscopy*," *Journal of Structural Biology*, 2013.
- M.Arjovsky, S.Chintala, and L.Bottou,"*Wasserstein generative adversarial networks*," in *International conference on machine learning*, 2017, pp. 214–223.
- V.M.Panaretos *et al*.,"*On random tomography with unobservable projection angles*," *The Annals of Statistics*, vol. 37, no. 6A, pp. 3272–3306, 2009.
- E. D. Zhong, T. Bepler, J. H. Davis, and B. Berger, "*Reconstructing continuous distributions of 3D protein structure from cryo-em images*," in *International Conference on Learning Representations*, 2020.
- A. Bora, E. Price, and A. G. Dimakis, "*AmbientGAN: Generative models from lossy measurements*." *ICLR*, vol. 2, p. 5, 2018.
- C.O.S.Sorzano, A.Jiménez, J.Mota, J.L.Vilas, D.Maluenda, M.Martínez, E.Ramírez- Aportela, T. Majtner, J. Segura, R. Sánchez-García *et al*., "*Survey of the analysis of continuous conformational variability of biological macromolecules by electron microscopy*," *Acta Crystallographica Section F: Structural Biology Communications*, vol. 75, no. 1, pp. 19–32, 2019.
- J. Andén, E. Katsevich, and A. Singer, "*Covariance estimation using conjugate gradient for 3d classification in cryo-EM*," pp. 200–204.
- A.Dashti, P.Schwander, R.Langlois, R.Fung, W.Li,A.Hosseinizadeh, H.Y.Liao, J.Pallesen, G. Sharma, V. A. Stupina *et al*., "*Trajectories of the ribosome as a brownian nanomachine*," *Proceedings of the National Academy of Sciences*, vol. 111, no. 49, pp. 17 492– 17 497, 2014.
- A.Moscovich, A.Halevi, J.Andén, and A.Singer,"*Cryo-em reconstruction of continuous heterogeneity by laplacian spectral volumes*," *Inverse Problems*, vol. 36, no. 2, p. 024003, 2020.
- R. R. Lederman, J. Andén, and A. Singer, "*Hyper-Molecules: on the Representation and Recovery of Dynamical Structures, with Application to Flexible Macro-Molecular Structures in Cryo-EM*," *Inverse Problems*, vol. 36, Apr. 2020.
- E.Seitz, F.Acosta-Reyes, P.Schwander, and J.Frank,"*Simulation of cryo-em ensembles from atomic models of molecules exhibiting continuous conformations*," *BioRxiv*, p. 864116, 2019.
- M.Unser, J.Fageot, and H.Gupta,"*Representer theorems for sparsity-promoting l_1- regularization*," *IEEE Transactions on Information Theory*, vol. 62, no. 9, pp. 5167–5180, Sep. 2016.
- L. Xu, J. S. J. Ren, C. Liu, and J. Jia, "*Deep Convolutional Neural Network for Image Deconvolution*," in Proceedings of the 27th International Conference on Neural Information Processing Systems, Cambridge, MA, USA, 2014, pp. 1790–1798.
- C. Dong, C. C. Loy, K. He, and X. Tang, "*Learning a Deep Convolutional Network for Image Super-Resolution*," in Computer Vision – ECCV 2014, 2014, pp. 184–199.

References

- K.H.Jin, M.T.McCann, E.Froustey,and M.Unser,"*Deep convolutional neural network for inverse problems in imaging*," *IEEE Trans. Image Process.*, vol. 26, no. 9, pp. 4509– 4522, 2017.
- Y.S.Han, J.Yoo, and J.C.Ye,"*Deep learning with domain adaptation for accelerated projection reconstruction MR*," arXiv:1703.01135 [cs.CV], 2017.
- S.Antholzer, M.Haltmeier, and J.Schwab,"*Deep learning for photoacoustic tomography from sparse data*," arXiv:1704.04587 [cs.CV], 2017.
- S.Wang, Z.Su, L.Ying, X.Peng, S.Zhu, F.Liang, D.Feng, and D.Liang,"*Acceleratingmag- netic resonance imaging via deep learning*," in *Proc. IEEE Int. Symp. Biomed. Imaging (ISBI)*, 2016, pp. 514–517.
- Lehtinen, J., Munkberg, J., Hasselgren, J., Laine, S., Karras, T., Aittala, M., & Aila, T. (2018). Noise2noise: Learning image restoration without clean data. *arXiv preprint arXiv:1803.04189*.
- Krull, A., Buchholz, T. O., & Jug, F. (2019). Noise2void-learning denoising from single noisy images. In *Proceedings of the IEEE Conference on Computer Vision and Pattern Recognition* (pp. 2129-2137).
- Heckel, R., & Hand, P. (2018). Deep decoder: Concise image representations from untrained non-convolutional networks. *arXiv preprint arXiv:1810.03982*.
- Karras, T., Laine, S., & Aila, T. (2019). A style-based generator architecture for generative adversarial networks. In *Proceedings of the IEEE conference on computer vision and pattern recognition* (pp. 4401-4410).
- Kingma, D. P., & Welling, M. (2013). Auto-encoding variational bayes. *arXiv preprint arXiv:1312.6114*.

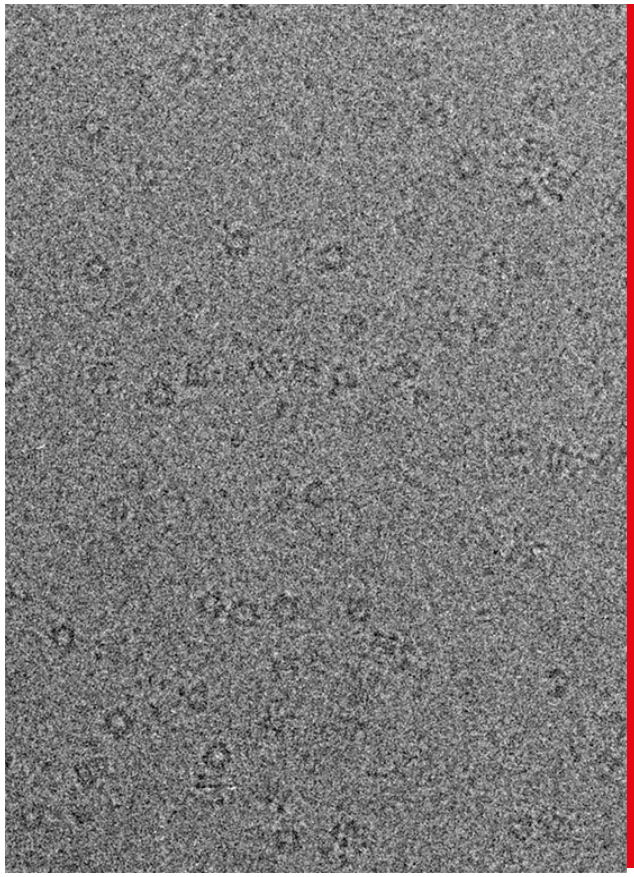

Thank you!
Questions?

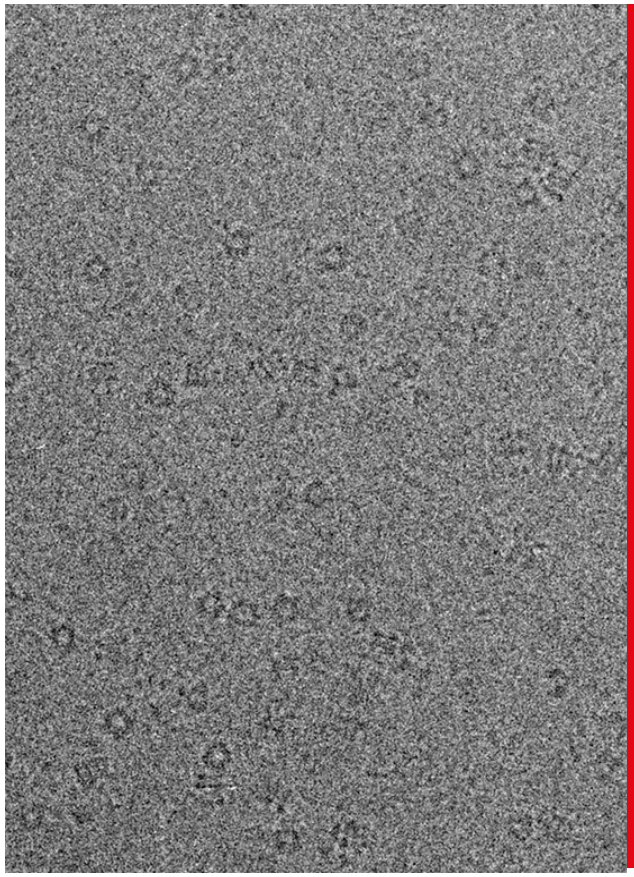

Appendix

CryoGAN vs Likelihood methods

- Max-likelihood

$$\mathbf{x}_{\text{rec}} = \arg\max_{\mathbf{x}} \sum_{n=1}^{N} \log p(\mathbf{y}^n_{\text{data}}|\mathbf{x})$$

- KL-Divergence

$$\mathbf{x}_{\text{rec}} = \arg\min_{\mathbf{x}} KL(p_{\text{data}}(\mathbf{y})||p(\mathbf{y}|\mathbf{x}))$$

$$\mathbf{x}_{\text{rec}} = \arg\min_{\mathbf{x}} \mathbb{E}_{\mathbf{y}\sim p_{\text{data}}}\left[\log \frac{p_{\text{data}}(\mathbf{y})}{p(\mathbf{y}|\mathbf{x})}\right]$$

Need to calculate $p(\mathbf{y}|\mathbf{x})$.

Wasserstein Distance

$$\mathbf{x}_{\text{rec}} = \operatorname{argmin}_{\mathbf{x}} \inf_{\gamma\in\Pi(p_{\mathbf{x}},p_{\text{data}})} \mathbb{E}_{(\mathbf{y}_1,\mathbf{y}_2)\sim\gamma}[\|\mathbf{y}_1 - \mathbf{y}_2\|]$$

$$\mathbf{x}_{\text{rec}} = \operatorname{argmin}_{\mathbf{x}} \max_{\mathbf{D}_\phi:\|\mathbf{D}_\phi\|_L<1} \left(\mathbb{E}_{\mathbf{y}\sim p_{\text{data}}}[\mathbf{D}_\phi(\mathbf{y})] - \mathbb{E}_{\mathbf{y}\sim p_{\mathbf{x}}}[\mathbf{D}_\phi(\mathbf{y})]\right)$$

Just require a sampler from the distributions

Theoretically both are the same (distributional matching) but one is explicit and one is implicit!!

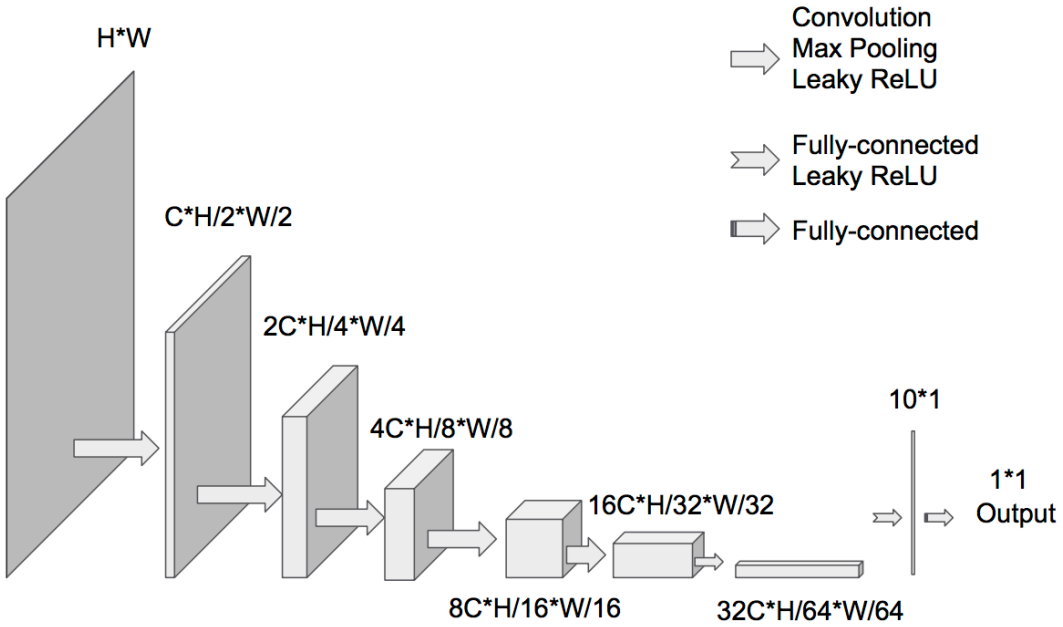
H*W
C*H/2*W/2
2C*H/4*W/4
4C*H/8*W/8
8C*H/16*W/16
16C*H/32*W/32
32C*H/64*W/64
10*1
1*1
Output
Convolution
Max Pooling
Leaky ReLU
Fully-connected
Leaky ReLU
Fully-connected

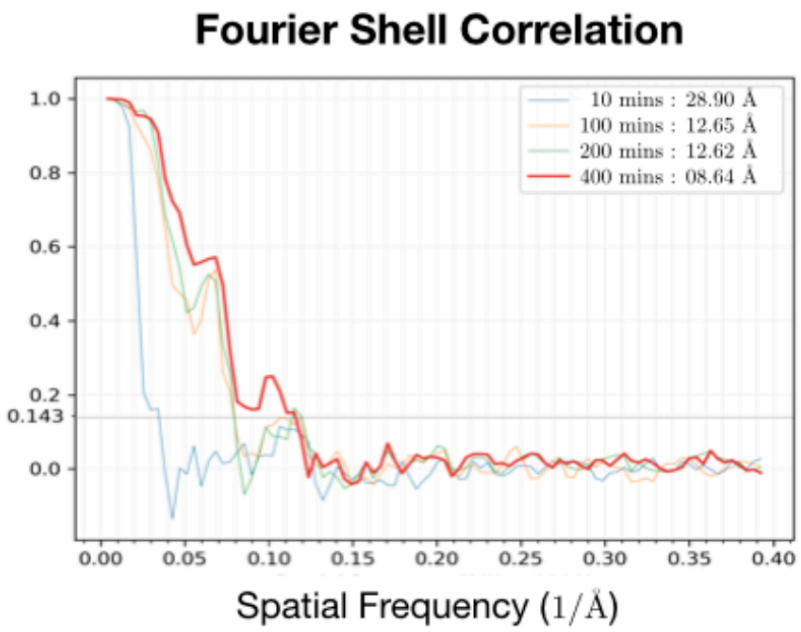
Fourier Shell Correlation
10 mins : 28.90 Å
100 mins : 12.65 Å
200 mins : 12.62 Å
400 mins : 08.64 Å
1.0
0.8
0.6
0.4
0.2
0.143
0.0
0.00
0.05
0.10
0.15
0.20
0.25
0.30
0.35
0.40
Spatial Frequency (1/Å)

TABLE I
RECONSTRUCTION RESOLUTION (Å) FOR SYNTHETIC β-GALACTOSIDASE

	SNR (dB), translation (%)			
metric	-20, 0	-5.2, 0	-20, 3	-20, 20
half-map FSC = 0.143	8.6	7.5	10.8	14.3
truth FSC = 0.5	15.3	8.3	14.7	23.2
truth FSC = 0.143	11.7	6.5	11.5	19.8

Pose Distribution Mismatch

TABLE II
RECONSTRUCTION RESOLUTION (Å) FOR β-GALACTOSIDASE

	reconstruction distribution		
true distribution	uniform	$\sigma = 2$	$\sigma = 3$
half-map FSC = 0.143			
uniform	8.6	13.2	17.2
$\sigma = 2$	9.2	9.4	14.7
$\sigma = 3$	8.6	10.6	12.7
ground truth FSC = 0.5			
uniform	15.3	16.1	18.6
$\sigma = 2$	16.4	15.0	15.5
$\sigma = 3$	16.4	16.9	16.1
ground truth FSC = 0.143			
uniform	11.7	12.6	14.5
$\sigma = 2$	11.6	10.4	10.7
$\sigma = 3$	11.5	14.0	12.3

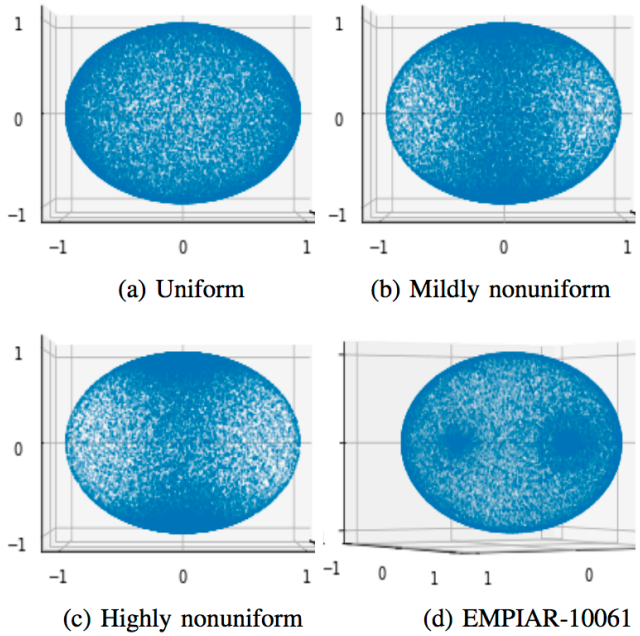

(a) Uniform (b) Mildly nonuniform

(c) Highly nonuniform (d) EMPIAR-10061

Fig. 7. Pose samples (40,000) from the pose distributions on a unit sphere used in the experiments. (a-c) are used to generate synthetic projection datasets from β-galactosidase. These are then again used in the simulator to reconstruct from each of these datasets. (d) is obtained from estimating poses for 108,209 particles picked from 1539 micrographs from EMPIAR-10061. The pose were estimated using the refinement step in RELION [9].

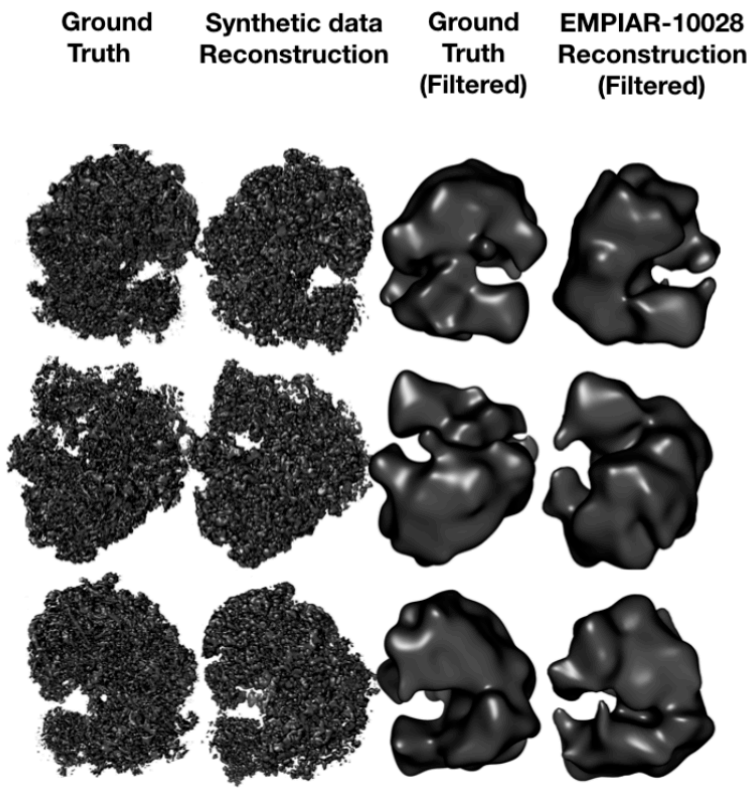
Ground Truth
Synthetic data Reconstruction
Ground Truth (Filtered)
EMPIAR-10028 Reconstruction (Filtered)

Neural Network Architecture

Layer ID	Layer	Resample	Output Shape (CxHxW)
1	Conv2d	MaxPool	96 × 16 × 16
2	Conv2d	MaxPool	192 × 8 × 8
3	Conv2d	MaxPool	384 × 4 × 4
4	Conv2d	MaxPool	768 × 2 × 2
5	Flatten	-	3072× 1 × 1
6	FC	-	50 × 1 × 1
7	FC	-	1 × 1 × 1

Layer ID	Layer	Resample	Norm	Output Shape (C, D, H, W)
1	Conv3d	-	BN	16 × 32 × 32 × 32
2	Conv3d	MaxPool	BN	16 × 16 × 16 × 16
3	Conv3d	-	BN	32 × 16 × 16 × 16
4	Conv3d	MaxPool	BN	32 × 8 × 8 × 8
5	Conv3d	-	BN	64 × 8 × 8 × 8
6	Conv3d	MaxPool	BN	64 × 4 × 4 × 4
7	Conv3d	-	BN	128 × 4 × 4 × 4
8	Conv3d	MaxPool	BN	128 × 2 × 2 × 2
9	Conv3d	-	BN	256 × 2 × 2 × 2
10	Conv3d	-	BN	256 × 2 × 2 × 2
11	Conv3d	Upsample	BN	128 × 4 × 4 × 4
12	Concat(layer 8)	-	-	256 × 4 × 4 × 4
13	Conv3d	-	BN	128 × 4 × 4 × 4
14	Conv3d	-	BN	128 × 4 × 4 × 4
15	Conv3d	Upsample	BN	64 × 8 × 8 × 8
16	Concat(layer 6)	-	-	128 × 8 × 8 × 8
17	Conv3d	-	BN	64 × 8 × 8 × 8
18	Conv3d	-	BN	64 × 8 × 8 × 8
19	Conv3d	Upsample	BN	32 × 16 × 16 × 16
20	Concat(layer 4)	-	-	64 × 16 × 16 × 16
21	Conv3d	-	BN	32 × 16 × 16 × 16
22	Conv3d	-	BN	32 × 16 × 16 × 16
23	Conv3d	Upsample	BN	16 × 32 × 32 × 32
24	Concat(layer 2)	-	-	32 × 32 × 32 × 32
25	Conv3d	-	BN	16 × 32 × 32 × 32
26	Conv3d	-	BN	16 × 32 × 32 × 32
27	Conv3d	-	BN	1 × 32 × 32 × 32

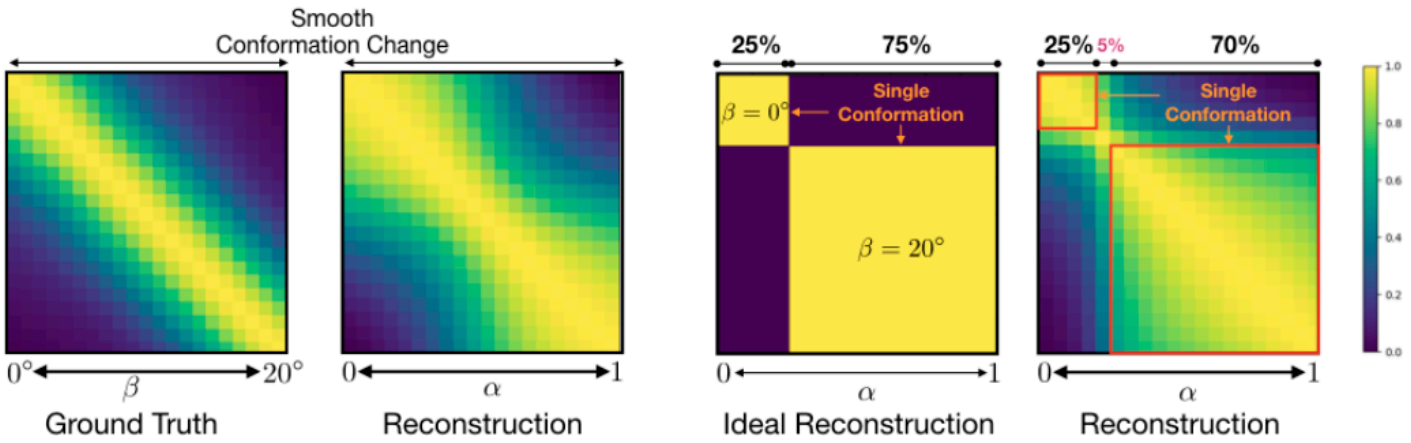

a. **Continuous Conformations (FSCCC Matrix)**

b. **Discrete Conformations (FSCCC Matrix)**